

## Research on Grinding Parameters of Parts with Same Clamping Mode and Different Sizes

Hua Zhang (0000-0002-9660-9536)<sup>1</sup>, Hua Chen (0000-0003-3217-0744)<sup>1</sup>, Lai Hu (0000-0002-7030-6721)<sup>1,2,\*</sup>

<sup>1</sup>School of Electrical and Electronic Engineering, Chongqing Vocational and Technical University of Mechatronics, Chongqing, China.

<sup>2</sup>School of Mechanical Engineering, Xi'an Jiaotong University, 28 Xianning Road, Xi'an, Shaanxi 710049, P.R. China. \*Corresponding e-mail: Lai Hu: Laifinial@163.com

**Aiming to study the influence of ultra-precision grinding parameters on the accuracy between the same clamping method and different workpiece sizes. This paper mainly analyzes the difference between the measurement precision of different parts by the same measurement method and the measurement precision of the same parts by different measurement methods. Therefore, the influence of grinding parameters on grinding precision is reflected. For the same part, it is concluded that the coaxiality error coincidence degree at end A and end B reaches 90.32% and 95.27%, respectively by using precision three-coordinate measuring instrument and Mahr roundness instrument. The coincidence degree of end A and end B verticality error reached 97.54% and 91.08%, respectively. For parts with different sizes, the Mahr roundness meter is used for measurement. The analysis shows that the coaxiality coincidence at end A and end B is the highest, reaching 98.36% and 92%, respectively. And from the analysis, the errors are mainly reflected in the factors such as jig and fixture and grinding process.**

**Keywords:** Ultra-precision/ultra-high speed grinding; Grinding parameters; Optimization; Precision error

### 1 Introduction

In the global machinery manufacturing industry, grinding is one of the most important links in the processing steps. When the workpiece is grinding, it is the final process. [1]. The accuracy of the final part and the stability of the precision depend on the grinding process. Therefore, the grinding process is particularly important. Ultra-precision and ultra-high speed grinding is one of the difficult problems in the machining industry. This difficulty mainly lies in the guarantee and stability of grinding precision. Many authors have also studied some contributions. For example, in the aspect of grinding precision control; Tawakoli T et al. [2] studied the influence of workpiece, and grinding parameters on minimum lubrication MQL grinding. The relationship between grinding parameters, grinding accuracy, and performance is analyzed from the perspective of abrasive microscopy. It is also concluded that the metal removal rate in MQL grinding is mainly affected by shear and fracture. Unlike conventional fluid grinding and dry grinding, plastic deformation, abrasive particle pullout and ploughing are not easy to occur.

Padda A S et al. [3] studied the influence of different surface grinding parameters on the surface roughness of stainless steel. The author analyzed the influence of cutting depth, grinding wheel speed and particle size on roughness when inputting grinding

parameters and using white alumina grinding wheel. The author thinks that the most influential factor in surface grinding is grinding wheel speed, followed by crystal particle size and cutting depth. Research on grinding parameters, Vishal Francis et. al. [4] stated that if feed and depth of cut were varied and spindle speed was kept constant to observe their effect on surface roughness. Then feed rate was found to be the most significant factor in case of cast iron and none of the factor was found be significant for mild steel and stainless steel. H. Adibi et. al. [5] stated that the amount of loading over the wheel surface increases sturdily with increasing depth of cut but is less affected by changes of table speed. Kirankumar R. Jagtap et. al. [6] stated that the most influencing parameter to surface roughness for AISI 1040 is work speed (Nw) in rpm followed by cutting depth, grinding wheel speed and number of passes. For the stability of grinding accuracy, grinding temperature is a very important factor. Alagumurthi N et al. [7] obtained better surface integrity of AISI3310, AISI6150 and AISI52100 steel materials by optimizing the calorific value during cylindrical grinding and establishing the temperature rise model between the grinding wheel and the workpiece contact area. Lan S et al. [8] measured the grinding temperature field of the workpiece at different depths with K-type thermocouple, and compared the analysis results with finite element method. The results show that the heat source model based on the temperature matching

method is basically consistent with the measured values at different depths. The relative error is between 1.8% and 8%. Compared with the triangular heat source model, the accuracy of the predicted temperature field distribution is improved by nearly 2 times. In addition to the above scholars' research on grinding, some scholars have conducted research [9-11]. In these scholars, few authors consider the most fundamental accuracy factor, that is, the relationship between measurement error and grinding parameters. Based on this research point, this study initially analyzed and modeled the grinding parameters by two ways both cylindrical grinding and inner grinding. The precision model is optimized by the neural network algorithm. At the same time, considering the same clamping mode of grinding parts, the geometric shape and position errors are analyzed for the same length, different diameter, and two measurement methods. The relationship between the two measurement methods and grinding parameters under different conditions is obtained.

$$E = \int_0^{t+H} P_{in} dt = \int_0^{t+H} \frac{P_{in}}{\eta(t)} = \int_0^{t+H} \frac{2\pi M_0 N + 4\pi^2 B S_n^2 + \alpha C_{F_c} S_p^{x_{F_c}} S_f^{y_{F_c}} (\pi d N) S_v^{Z_{F_c}+1} K_{F_c}}{(1000 \times i)^{S_v^{Z_{F_c}}} \eta(t)} dt \quad (1)$$

Where:

$t$  ... Number of grinding times,

$H$  ... Number of light grin,

$M_0$  ... Non-load Coulomb friction resistance moment equivalent to the spindle motor shaft of the grinder main transmission system,

$B$  ... Viscous friction damping coefficient of the grinding machine main transmission system equivalent to the motor spindle,

$\omega$  ... Angular velocity of the motor spindle,

$\alpha$  ... Load factor of the mechanical transmission system,

$N$  ... Rotate speed of the spindle motor,  $S_v = N/i$ ,

$S_v$  ... Cutting speed,  $S_v = \pi d Z_n / 1000$ ,

$Z_n$  ... Spindle speed,

$C_{F_c}$  ... Influence coefficient of cutting force, which is related to the material and processing conditions of the workpiece to be processed,

$Z_{F_c}$  ... Exponential coefficient of cutting speed  $S_v$ .

## 2.2 Optimize parameters

According to the analysis in this paper, neural network is used to optimize this. BP (Back Propagation Network) neural network is a multi-layer feedforward neural network, which consists of input layer, hidden layer and output layer [15-16]. Before optimization, it is necessary to design an optimization model for the whole grinding parameters. The model is shown in Equation (14). Initially, the energy consumption model (Eq. 1) is imported into the MATLAB neural network optimization interface. Constraints are applied (Eq.14). Set

## 2 Multi-objective optimization model of grinding parameters

In ultra-precision/ultra-high speed grinding, besides considering the influence of equipment's precision, it is more important to select grinding parameters. Aiming to facilitate the research, the parametric precision modeling is mainly carried out for different diameters under the same clamping methods and size parts. Therefore, the differences of grinding parameters of two diameters are compared and analyzed.

### 2.1 Objective function

In this study, the energy consumption of the grinding machine is the lowest on the premise of ensuring the accuracy. Therefore, high precision and low energy consumption are optimized for multi-objective functions. High precision is expressed by  $A_{CC}$ . Energy consumption is represented by  $E$ . Meanwhile, according to the manual query and establish the energy consumption objective function:

the initial value of the outer circle [30, 30, 30, 1.5, 1, 15, 18, 80], the minimum value of the outer circle parameter [25, 25, 20, 1, 1, 11, 15, 70], and the maximum value of the outer circle parameter [40, 40, 40, 3, 3, 20, 25, 120]. At the same time, the initial value of the inner circle [30, 30, 30, 1.5, 1, 15, 18, 80], the minimum value of the inner circle parameter [25, 15, 20, 1, 1, 11, 15, 70] and the maximum value of the inner circle parameter [40, 30, 40, 3, 3, 20, 25, 130] are also set. Finally, the optimal grinding rounding parameters are shown in Tab. 1.

$$\begin{aligned} \min F(S_{n_{\max}}, S_{v_{\min}}, S_p, S_f, P_{\max}, P_{s_n}, Z_n) &= \{\max A_{CC}; \min E\} \\ \left\{ \begin{array}{l} S_{n_{\min}} \leq S_n \leq S_{n_{\max}} \\ S_{v_{\min}} \leq S_v \leq S_{v_{\max}} \\ S_{p_{\min}} \leq S_p \leq S_{p_{\max}} \\ S_{f_{\min}} \leq S_f \leq S_{f_{\max}} \\ 1 \leq H \leq 3 \\ \frac{C_{F_c} a_p^{x_{F_c}} f^{y_{F_c}} K_{F_c}}{\eta} \left( \frac{\pi d N}{1000 \times i} \right)^{n_{F_c}+1} \leq P_{\max} \\ a S_n / i + b \leq P_{s_n} \\ Z_{n_{\min}} \leq Z_n \leq Z_{n_{\max}} \end{array} \right. \quad (2) \end{aligned}$$

Where:

$S_n$  ... Grinding wheel speed,

$S_v$  ... Grinding speed,

$S_p$  ... Grinding depth,

$S_f$  ... Feed,

$H$  ... Light grinding times,

$P$  ... Grinding power,

$P_{SA}$  ... Spindle acceleration power,

$Z_n$  ... Workpiece spindle speed.

**Tab. 1** Optimal parameters of outer circle and inner hole

Outer circle				Inner bore			
Variable	Initial value	Scope	Results	Variable	Initial value	Scope	Results
$S_n$ (m/s)	30	25-40	30	$S_n$ (m/s)	30	25-40	35
$S_v$ (mm/min)	30	25-40	25	$S_v$ (mm/min)	20	15-30	18
$S_p$ (um)	30	20-40	25	$S_p$ (um)	30	20-40	35
$S_f$ (um)	1.5	1-3	1.6	$S_f$ (um)	1.5	1-3	1
$H$	1	1-3	3	$H$	1	1-3	3
$P$ (KW)	15	11-20	16	$P$ (KW)	15	11-20	15
$P_{SA}$ (KW)	18	15-25	23	$P_{SA}$ (KW)	18	15-25	22
$Z_n$ (r/min)	80	70-120	90	$Z_n$ (r/min)	80	70-130	120

### 3 Test analysis

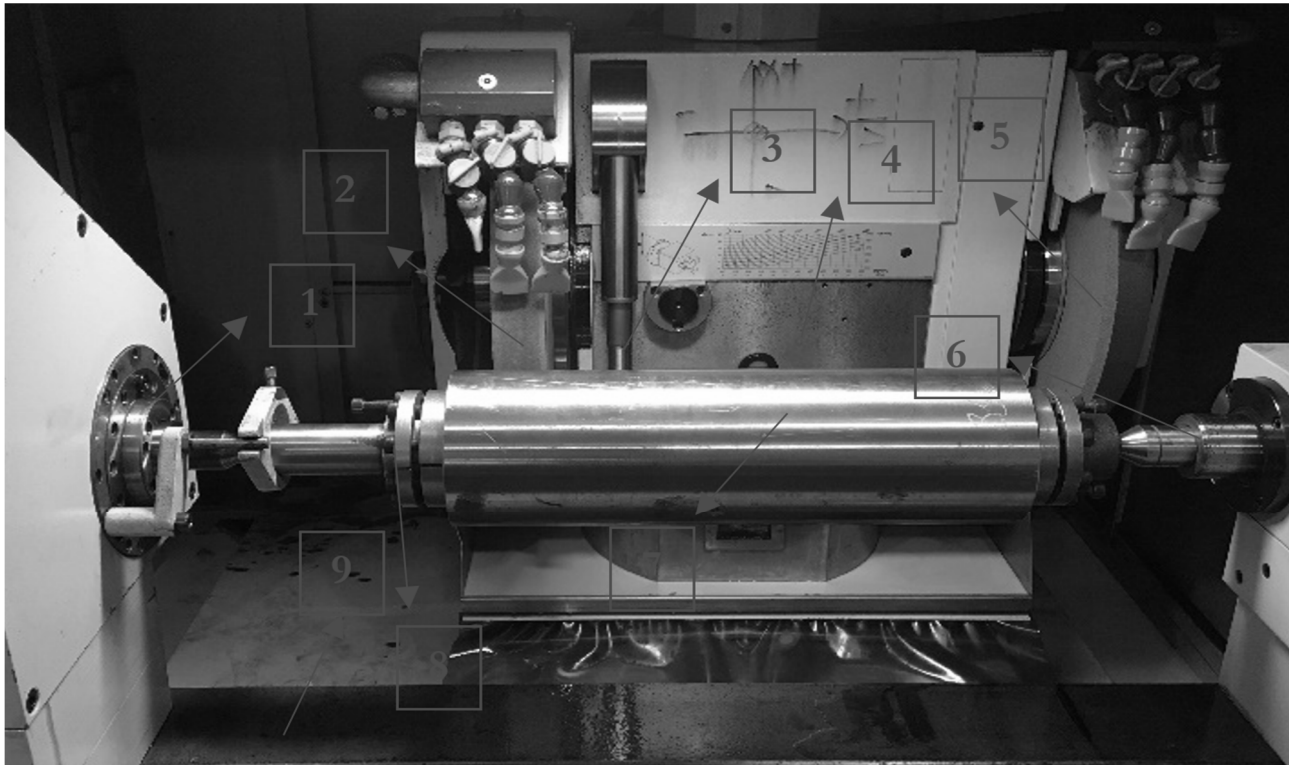
#### 3.1 Test results of precision three coordinate measurement method

The optimized results of grinding parameters are set so that the parts with the same length and different

diameters can be processed, respectively. Because this study mainly studies the parameters of high-precision grinder. The machine is Kellenbergaer universal grinder from Switzerland, and the detailed grinding parameters are shown in Tab. 2. The processing site is shown in Fig. 1.

**Tab. 2** Detailed grinding parameters

Project	Parameters
Grinding machine	Machining precision / 0.2 $\mu$ m
CBN wheel	Granularity: 270/325; Diameter: 700 mm; Binder concentration: 150%
Grinding depth / $a_p$	0.005 mm
Grinding wheel linear velocity / $v_s$	30000 mm/s
Workpiece speed / $v_w$	30 mm/s
Workpiece material	45#
Cooling mode	Wet grinding

**Fig. 1** Actual machining site of motorized spindle

Where:

- 1...Workpiece C axis,
- 2...Cylindrical grinding wheel,
- 3...Ruby probe,
- 4...Axis B,
- 5...30 ° end face grinding wheel,
- 6...Tailstock,
- 7...Motorized spindle part,
- 8...Tooling fixture,
- 9...Guide Rail.

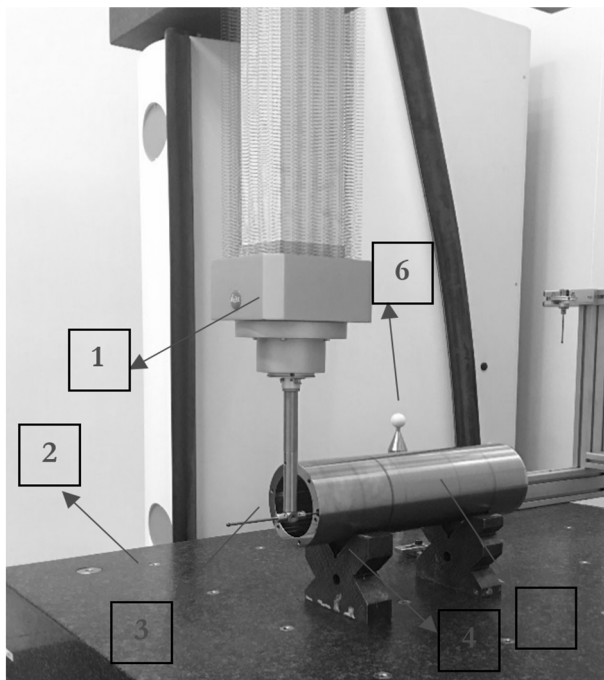


**Fig. 2** Inspection site of motorized spindle

**Tab. 3** Detection accuracy error table

Test items	Error/ $\mu\text{m}$	Test items	Error/ $\mu\text{m}$
End face 3 jumping	7.2	Internal bore surface 1 for the first time	20.1
End face 4 runout	8.4	Inner bore surface 1 second time	19.5
A verticality of end face	3	Inner bore surface 1 third time	5.6
B verticality of end face	4.5	Internal bore surface 2 for the first time	15.8
A end coaxiality	2.6	Inner bore surface 2 second time	11.6
B end coaxiality	1.2	Inner bore surface 2 third time	5.5

### 3.2 Test results of Mahr roundness meter

Aiming to verify the accuracy of the above processing and testing and analyze the causes of the largest errors. At the same time, self-test and evaluation of measuring instruments are carried out. Therefore, two different sizes of large and small diameter are measured again. This measuring instrument adopts Mahr roundness meter with a measuring precision of 0.01  $\mu\text{m}$ . Meanwhile, the maximum error generate for the results of Fig. 2 and Tab. 3 is the coaxiality error. Therefore, this measurement only measures coaxiality and verticality, thus making comparative analysis. The measurement site of Mahr roundness meter is shown in Fig. 3. The measurement curve of large diameter is

Where:

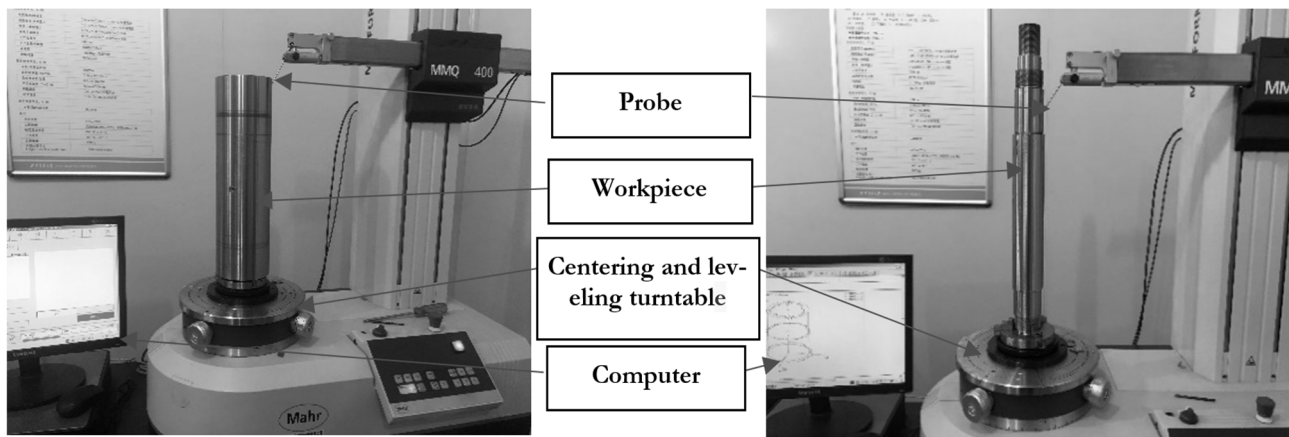
- 1...Telescopic probe,
- 2...Workbench,
- 3...Probe,
- 4...V block,
- 5...Motorized spindle part,
- 6...School team coordinate system.

As shown in Fig. 1, the part has no positioning stepped shoulder. So it is clamped and processed in a two-top way. Parts with small diameter and the same length are processed by the same clamping method. And a large diameter part is randomly taken and measured by Laitz precision three coordinates. The precision of the measuring instrument is 0.01  $\mu\text{m}$ . The measurement site is shown in Fig. 2. The measurement results are shown in Tab. 3.

Referring to the test results in Fig. 2 and Tab. 3, it can be clearly seen that the coaxiality of end face A is the maximum, reaching 2.6  $\mu\text{m}$ . At the same time, it can be seen from the data at both ends of A and B measurements that the precision gradually increases with the measurement depth, with the highest accuracy reaching 5.5  $\mu\text{m}$ . The reason is that the parts in the processing of the use of two—top processing, and the use of both ends is the way of positioning. Therefore, fixture errors will occur, which will eventually affect the overall part errors. Although these relevant data are obtained, aiming to avoid measurement errors during measurement, and to better verify the accuracy of data. The second measurement had been adopted for parts.

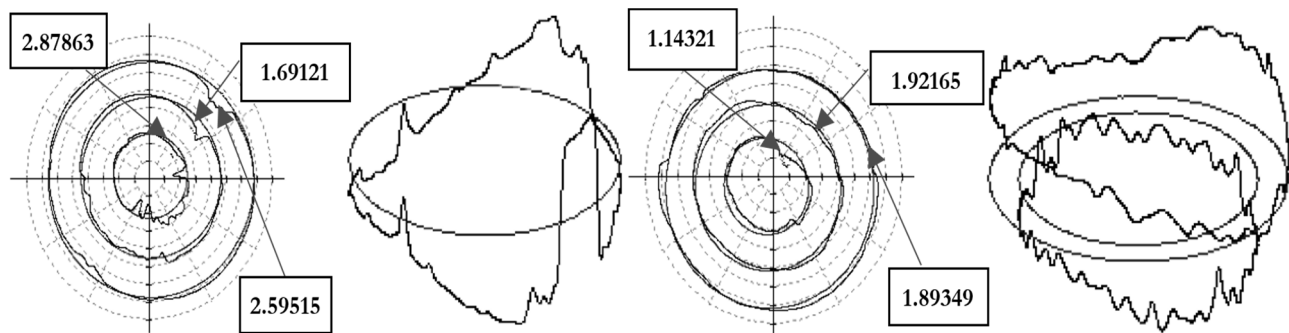
shown in Fig. 4. The small diameter measurement curve is shown in Fig. 5.

According to Fig. 4, the error of three-segment data at the end A is greater than the end B. As can be seen from the right view of Figs 4 (a) and (b), the sharp jump of Fig. 4 (a) is very obvious. For Fig. 5, the jumping range shown in the measurement drawings of the six small diameter parts at each measuring position is within 3  $\mu\text{m}$ . Using the same machining and clamping method, compared with large diameter parts, machining without inner holes will have higher precision than inner holes. Meanwhile, it is also reflected in the processing of parts with inner holes, and the processing and clamping method adopted is particularly important.



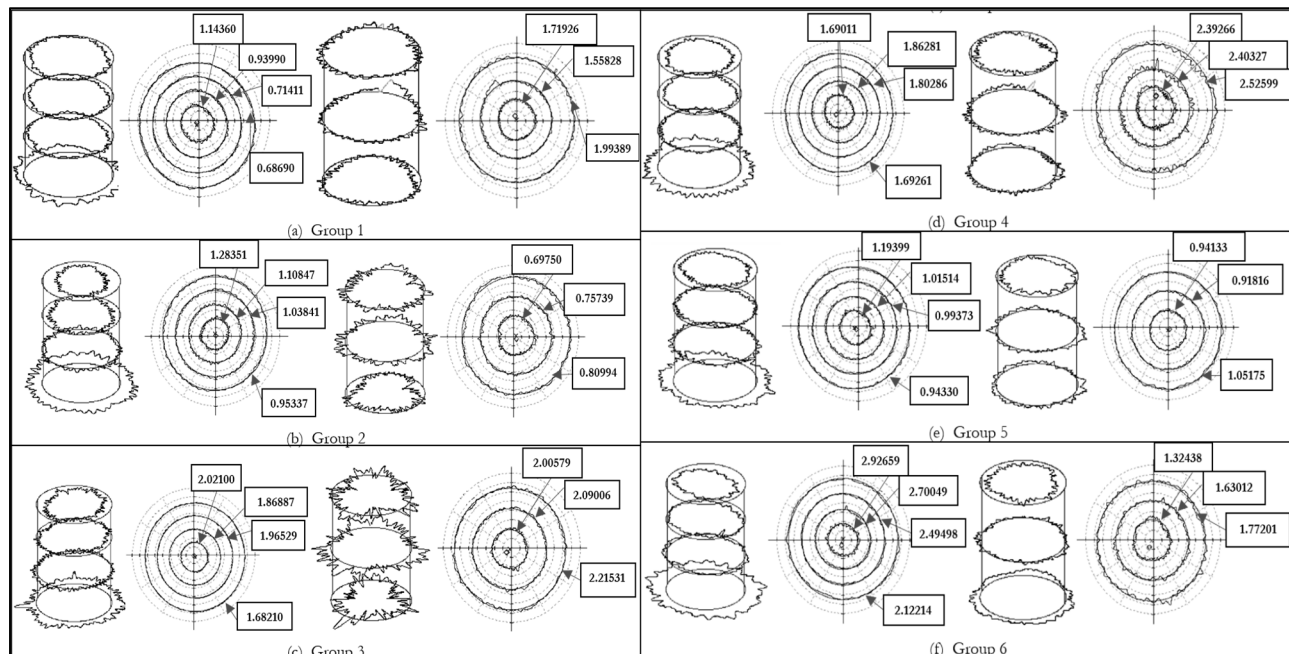
(a) Large diameter measurement

(b) Small diameter measurement

**Fig. 3** Field diagram of different parts measured by Mahr roundness meter

(a) A-end section

(b) B-end section

**Fig. 4** Large diameter measurement graph**Fig. 5** Small diameter measurement graph

#### 4 Test comparative analysis

In order to analyze the same measuring tool more intuitively, the measurement data of the two parts are

analyzed, separately. The precision errors of large diameter parts tested by Mahr roundness meter are shown in Tab. 4. The results of small diameter parts are shown in Tab. 5.

**Tab. 4** Large diameter measurement results

Measuring items	Error ( $\mu\text{m}$ )	Measuring items	Error ( $\mu\text{m}$ )
Cylindricity A	5.36336	Cylindricity B	5.89548
Cylindricity A	2.92617	Cylindricity B	4.94096
Verticality A	2.87863	Verticality B	1.14321
Cylindricity a1	2.59515	Cylindricity b1	1.14321
Cylindricity a2	1.69121	Cylindricity b2	1.92165
Cylindricity a3	2.87863	Cylindricity b3	1.89349

**Tab. 5** Measurement results of small diameter accuracy

Parts	Part 1	Part 2	Part 3	Part 4	Part 5	Part 6
Name						
Cylindricity 1( $\mu\text{m}$ )	1.97570	3.22648	3.39043	3.24805	2.38783	2.73368
Cylindricity 2( $\mu\text{m}$ )	2.02215	1.97227	1.14778	1.60017	1.85256	1.74539
CoaxialityA( $\mu\text{m}$ )	1.14360	2.92659	1.28351	2.02100	1.86281	1.19399
CoaxialityB( $\mu\text{m}$ )	1.99389	1.77201	0.80994	2.21531	2.52599	1.05175

Through the data analyzed in Tabs. 3-5, for the same part, the measurement results using precision three-coordinate measuring instrument and Mahr roundness instrument shown that the coaxiality error coincidence degree at ends A and B reaches 90.32% and 95.27%, respectively. The coincidence degree of ends A and B verticality error reached 97.54% and 91.08%, respectively. However, for parts with different sizes, Mahr roundness meter is used for measurement. The results shown that the coaxiality coincidence at ends A and B is 98.36% and 92%, respectively. By comparing the average data Tab. 5 with Tab. 4, the coaxiality coincidence between ends A and B only reaches 60.39% and 66.15%. Moreover, it is also concluded from Tabs. 4-5 that for parts of the same size, the two measurements have only slight errors, which are about 0.1-0.5  $\mu\text{m}$ . With the same clamping method, the error of 6 parts processed is between 0.1  $\mu\text{m}$  and 1.5  $\mu\text{m}$ . Therefore, it is analyzed that the vast majority of errors are reflected in factors such as jig and fixture and grinding process.

## 5 Conclusion

(1) This study mainly analyzes the influence of grinding precision through the analysis of different size parts, the same measurement methods and different measurement methods in the same machining clamping method. Before the analysis and comparison, the neural network is used to optimize the variables of the grinding parameter model designed and analyzed. The optimal data are obtained for setting and grinding, and finally different measurements are carried out on the machined parts.

(2) In the process of measurement, two measuring instruments are used. According to the analyzed of the test results, for the same part, two measurement methods are adopted, and the coaxiality error coincidence degree at the A ends and B reaches 90.32% and 95.27%, respectively. The coincidence degree of ends

A and B verticality error reached 97.54% and 91.08%, respectively. However, for parts with different sizes, Mahr roundness meter is used for measurement. The results shown that the coaxiality coincidence at ends A and B is 98.36% and 92%, respectively. Through further processed and analyzed of the data, using the same measuring instrument to analyzing and comparing the average data measured by different parts, the coaxiality coincidence degree between end A and end B only reaches 60.39% and 66.15%. Meanwhile, it is also concluded that with the same size of parts, the two measurements have only slight errors, about 0.1  $\mu\text{m}$ -0.5  $\mu\text{m}$ . For the analyzed of measurement data of 6 small diameters, the error is between 0.1  $\mu\text{m}$  and 1.5  $\mu\text{m}$ .

(3) Based on the analysis of data and energy saving, the majority of errors are reflected in the level of tooling and fixture, and grinding process. This also guides us in ultra-precision grinding, grinding parameters have a great influence on grinding accuracy, and measurement accuracy will also account for a certain proportion. When the error is 0.1  $\mu\text{m}$ -0.5  $\mu\text{m}$  or 0.1  $\mu\text{m}$ -1.5  $\mu\text{m}$ , the energy consumption cost can be greatly reduced by reasonably selecting the allowance for finishing and grinding parameter variables. It can also be revealed that more specific allowance for finishing can be obtained when different combinations of 8 grinding parameters are selected in high precision grinding. Its ultimate aim is to reduce energy consumption and improve workpiece quality and machining accuracy. This is also the specific work to be done in the future: forming a micro-system for selecting grinding parameters in the field of ultra/high precision grinding.

## Acknowledgement

*This research was funded by the Chongqing Education Commission Science and Technology Research Project(KJZD-K201903701) and*

**(KJQN201803703) and the Chongqing Higher Education Teaching Reform Research Project (193463).**

## References

- [1] CHANG Z, HU L. (2021). Study on scatter of surface integrity of bearing raceway grinding[J]. *Manufacturing Technology*, 21(6):781-787
- [2] TAWAKOLI T., HADAD M. J., SADEGHI M. H. (2009). An experimental investigation of the effects of workpiece and grinding parameters on minimum quantity lubrication—MQL grinding[J]. *International Journal of Machine Tools & Manufacture*, 49(12-13):924-932
- [3] PADDA A. S., KUMAR S., MAHAJAN A. (2015). Effect of Varying Surface Grinding Parameters on the Surface Roughness of Stainless Steel[J]. *Carbon*, 100: 0.08
- [4] VISHAL FRANCIS, ABHISHEK KHALKHO, JAGDEEP TIRKEY, ROHIT SILAS TIGGA & NEELAM ANMOL TIRKEY. (2014). Experimental Investigation And Prediction Of Surface Roughness In Surface Grinding Operation Using Factorial Method And Regression Analysis [J]. *International Journal of Mechanical Engineering And Technology (IJMET)*, Volume 5, Issue 5, May, pp. 108-114
- [5] ADIBI H., REZAEI S. M., SARHAN A. A. D. (2013). Analytical modeling of grinding wheel loading phenomena[J]. *The International Journal of Advanced Manufacturing Technology*, 68(1-4): 473-485
- [6] JAGTAP K. R., UBALE S. B., KADAM M. S. (2011). Optimization of cylindrical grinding process parameters for AISI 5120 steel using Taguchi method [J]. *International Journal of Design and Manufacturing Technology*, 2(1): 47-56
- [7] ALAGUMURTHI N., PALANIRADJA K., SOUNDARARAJAN V. (2007). Heat generation and heat transfer in cylindrical grinding process -a numerical study [J]. *International Journal of Advanced Manufacturing Technology*, 34(5-6):474-482
- [8] LAN S., JIAO F. (2019). Modeling of heat source in grinding zone and numerical simulation for grinding temperature field [J]. *International Journal of Advanced Manufacturing Technology*, 103(15)
- [9] KHRAMENKOV M, JERSÁK J. (2021). Effect of the dressing process on the surface roughness in cylindrical grinding of Ti6Al4V alloy using stationary diamond dressing tools [J]. *Manufacturing Technology*, 21(5):640-646
- [10] FARSKÝ J, ZETEK M, BAKŠA T, KUBÁTOVÁ D, HU Y. (2020). Effect of the cutting conditions on surface roughness during 5-axis grinding of Maraging steel MS1 [J]. *Manufacturing Technology*, 20(1)
- [11] SALONITIS K., CHONDROS T., CHRYSSOLOURIS G. (2008). Grinding wheel effect in the grind-hardening process [J]. *The International Journal of Advanced Manufacturing Technology*, 38(1-2): 48-58
- [12] YU X. (2011). Finite element analysis of influence of grinding parameters on grinding force[C]// *International Conference on Electronic & Mechanical Engineering & Information Technology*. IEEE
- [13] LI L., CHEN B., CHEN B. (2015). Multi-objective optimization of cutting parameters in sculptured parts machining based on neural network [J]. *Journal of Intelligent Manufacturing*, 26(5):1-8
- [14] MAYER J. E., FANG G. P. (1995). Effect of Grinding Parameters on Surface Finish of Ground Ceramics [J]. *CIRP Annals - Manufacturing Technology*, 44(1):279-282
- [15] BEYER H. G. (1999). The simple genetic algorithm: foundations and theory [M]. 1999
- [16] TANG L., YUAN S., TANG Y. (2019). Optimization of impulse water turbine based on GA-BP neural network arithmetic [J]. *Journal of Mechanical Science and Technology*, 33(1):241-253